



DEVELOPING RISK-TARGET BASED DESIGN APPROACHES FOR BASE-ISOLATED BUILDINGS

*A. Flora⁽¹⁾, G. Perrone⁽²⁾, D. Cardone⁽³⁾

⁽¹⁾ Research Fellow, School of Engineering, University of Basilicata, amedeo.flora@unibas.it

⁽²⁾ Postdoctoral Fellow, School of Engineering, University of Basilicata, giuseppe.perrone@unibas.it

⁽³⁾ Associate Professor, School of Engineering, University of Basilicata, donatello.cardone@unibas.it

Abstract

Most of current seismic codes allow engineers to design seismic resistant structures with a certain amount of safety with respect to the onset of given limit states (such as serviceability, life safety or collapse). In such approach, the effective risk toward selected limit states is not explicitly considered. Unknown values of failure probability are then implicitly accepted. Moreover, the resulting risk is not constant among different structural types and/or locations.

Recently, a number of risk-target design procedures have been proposed for fixed-base buildings, in order to achieve a given uniform risk level for the structure. Such procedures have been also implemented in advanced seismic codes (e.g. ASCE7-10 and in ASCE7-16). So far, specific risk-target based design approaches for base-isolated buildings are missing. In this context, the results of the RINTC (Implicit Risk of code-conforming Italian buildings) research project, funded within the ReLuis/DPC 2015-2018 research program, outlined that, despite the compliance with the minimum requirements of the Italian seismic code ensure the acceptable level of safety, the resilience objective suggested in other international seismic codes is not fully guaranteed for base-isolated buildings, especially in high seismicity regions. In this paper, a Risk-Target Based Design (RTBD) approach for base-isolated buildings is presented. The effect of different sources of uncertainty (record-to-record, modeling assumptions and limit state definition) is taken into account. The proposed approach is then applied to a selected case-study, representative of typical Italian residential RC building equipped with rubber-based isolation systems (High Damping Rubber Bearings (HDRBs) plus Friction Slider Bearings (FSBs)). In order to validate the proposed approach, Multiple Stripe Analyses (MSA) are performed, to evaluate the actual risk associated with the designed building. Based on the results of this study, some preliminary conclusions oriented towards current practice are drawn, i.e.: an acceptable risk can be attained assuming a behavior factor equal to 1 for the superstructure and increasing by approximately 20% the design displacement of the isolation system derived by applying the Italian seismic code.

Keywords: risk-target based design, high damping rubber bearings, multiple-stripe analyses, non-linear models.

1. Introduction

Generally, modern seismic codes are focused on ensuring the achievement of one or more design objectives, expressed in terms of engineering limit state (such as the serviceability or life safety), for a certain intensity level (Return Period). The latter approach, carried out using an uniform-hazard spectrum for a fixed return period, does not explicitly consider risk and also neglects many sources of uncertainty (record-to-record, modeling ecc.). As a consequence, unknown values of the failure probability are implicitly accepted and the risk is not constant among different structural types and/or locations. In other words, designing different buildings for a given, uniform ground motion hazard, does not assure that the level of risk is the same but only that the structure is “code-conforming” [1].

In the optic of an uniform-risk based design of structures, Luco et al. [2] proposed a systematic design approach based on the use of fixed, theoretical (generic) collapse fragility functions and on the definition of location-specific risk factors. The mentioned risk factors are defined as the ratio between the design ground motion level that guarantees an “acceptable” risk and the design ground motion level prescribed by the code (e.g., that exceeded with 10% chances in 50 years). In the study of Luco et al., a collapse rate of 2×10^{-4} (i.e.,



1% probability in 50 years, corresponding to the “average risk” observed in the US territory) is assumed as an “acceptable” risk level.

Luco et al. derived Risk-Targeted (RT) design maps expressed in terms of risk factors. Such maps are currently adopted in ASCE7-10 [3] and in ASCE7-16 [4]. The same approach with different assumptions on collapse fragility and target collapse rates has been carried out in several studies [5, 6]. However, the mentioned studies are affected by a number of limitations. First of all, the obtained results appear strongly affected by the preliminary assumptions in terms of (collapse) fragility function and target (collapse) risk rates. The sensible differences among the target (collapse) risk values adopted in the proposed studies are representative of the lack of a common line, in the international scientific community, on this matter. Moreover, the RT approach is not able to guarantee an exact risk matching for any limit-state. Finally, a single design spectrum, although adjusted, cannot simultaneously cater to the needs of multiple different structures at a given site and only a fairly good risk harmonization with similar risk values can be achieved among different buildings and sites. In this context, the results of the RINTC (Implicit Risk of code-conforming Italian buildings) research project [7], funded within the ReLuis/DPC 2015-2018 research program, showed that the collapse risk of different building types at different locations is far from uniform, even for locations with identical design intensity level. In particular, the collapse rates increase with increasing values of the site hazard, namely the higher is the hazard the higher is the collapse rate [1]. Another interesting outcome is that base-isolated structures show lower “residual resistance” after the attainment of the design intensity level (hence higher collapse rate) than similar buildings in the fixed-base configuration, especially for high seismicity areas and for isolation systems based on High Damping Rubber Bearings (HDRBs). In the first part of this paper, the main outcomes of the RINTC project relevant to base-isolated buildings [7] are shown. In the second part, the theoretical basis of a Risk-Target Based Design (RTBD) approach for buildings with seismic isolation, equipped with hybrid systems (i.e. High Damping Rubber Bearings (HDRBs) plus Friction Slider Bearings (FSBs)), are summarized. The RTBD approach is applied to a selected case study representative of typical Italian residential RC buildings, assuming a target collapse rate of 2×10^{-4} . Multiple Stripe Analysis (MSA) are then performed to validate the envisaged RTBD approach for base-isolated buildings. Finally, some remarks on the implications of the results of this study for practical applications are discussed.

2. Revision of past results

The main aim of the ReLuis-DPC 2015-2018 RINTC research project [7] was the estimation of the probability of exceedance of a given performance levels (including global collapse) for different structural types (reinforced concrete, masonry, steel and base isolated structures). In the present study, reference to the Case 2-A [7], examined within the RINTC research project, has been made. The mentioned building has been designed according to the Italian Seismic Code [8] through Modal Response Spectrum Analysis (RSAs). The superstructure of the selected case-study is represented by 6-storeys RC frame building for residential use, located in L’Aquila, Soil C [7]. It features a regular plan of 240 square meters and an interstorey height equal to 3.05m (except for the ground level, which is 3.4m). The building is characterized by four frames in the long (X-) direction and six external frames in the short (Y-) direction. The staircase has been designed using knee beams. Cross-section dimensions and reinforcement ratios of beams and columns can be found in [7]. The masonry infill panels are regularly distributed (in plan and elevation) and are realized with hollow clay bricks of 300mm thickness, with different percentages of openings. An average cylindrical compressive strength of 28MPa has been assumed for concrete (concrete class C28/35). Similarly, a yield strength of 430MPa has been assumed for steel reinforcement (steel class B450C). The examined building is equipped with an hybrid isolation system composed by 16 HDRBs (equivalent viscous damping ratio equal to 15%), arranged below the perimeter columns of the building, and 8 FSBs (friction coefficient equal to 1%), arranged below the inner columns. Table 1 (first line) summarizes the main characteristics of the isolation system designed within the RINTC project, including the isolation ratio (fundamental period of the base-isolated building, T_{iso} , divided by that of the same building in the fixed-base configuration, T_{fb}). More details about the described case-study can be found in [7].



The nonlinear 3D model of the building structure has been developed using the structural analysis software framework OpenSees [9]. A lumped plasticity model has been chosen for the frame elements (beams and columns) of the superstructure. The Ibarra-Medina-Krawinkler [10] model has been assumed to describe the flexural behavior of the plastic hinges. In particular, the skeleton curves of such plastic hinges have been calibrated based on moment-curvature analysis of the critical cross sections of beams and columns, taking into account axial load interaction effects. For RC members liable to premature shear failure (like the short columns of the stairs), a fictitious ultimate rotation capacity has been defined. Masonry infill panels are modeled with an equivalent compression-only strut. The skeleton curves are derived according to a modified version of the Decanini model [7]. The influence of openings (windows or doors) in masonry infills has been taken into account by a proper reduction of their strength and lateral stiffness. In addition, the possibility of premature out-of-plane collapse of the infill has been taken into account.

Table 1 – Main characteristics of the isolation systems designed within the RINTC project (first line) and using the RTBD approach (second line) for the considered case-study building.

Case Study	Isolation System	HDRB*						FSB*			T _{iso} (sec)	T _{iso} /T _{fb}
		G (MPa)	ξ	V ₂ (kN)	D (mm)	t _e (mm)	d _c (mm)	V ₂ (kN)	d _c (mm)	μ		
RINTC	16HDRB+8FSB	0.4	15%	880	600	176	350	3500	350	1%	3.04	3.27
RTDB	16HDRB+8FSB	0.4	15%	820	650	207	400	3500	450	1%	3.04	3.27

* G: Dynamic shear modulus of rubber; ξ : equivalent damping ratio; V₂: Maximum gravity load capacity at the displacement d_c; d_c: Maximum displacement capacity of HDRB/FSB; D: Diameter of HDRB; t_e: Total thickness of rubber layers; μ friction coefficient of FSB at the maximum vertical load capacity

In the first part of the ReLuis-DPC 2015-2018 RINTC research project [7] the HDR Bearing Element [11] has been adopted to describe the cyclic behavior of HDRBs. This is a two-node element with 12 degrees-of freedom characterized by easy implementation and computational efficiency. The behavior in the axial direction captures the cavitation (occurring at a tensile force value producing a tensile stress of 3G) and post-cavitation behavior in tension as well as the variation of the critical buckling load and the vertical axial stiffness with horizontal displacement in compression. The bidirectional model proposed by Grant et al. [11] is adopted to describe the behavior in the two shear directions. The coupling between vertical and horizontal directions is partially taken into account in an indirect way by using expressions for mechanical properties in the vertical direction that are dependent on the response parameters in the horizontal direction. More details about the described model can be found in [7]. However, in the current version of the model, properties in the horizontal direction do not depend on the response in the vertical direction, neither for large displacements nor for large pressures. Therefore, the axial-shear load interaction as well as P-delta effects due to post buckling behavior are missed. As a consequence, in the second edition of the mentioned research project [12], the mechanical model of the HDRBs has been reviewed to better capture the axial shear load interaction at small and large displacements as well as pre and post-buckling behavior. In particular, the Kikuchi Bearing Element [13] has been considered in lieu of the HDR bearing model. The Kikuchi bearing element is a two node link element with multi-spring mechanical model which includes two sets of multiple axial springs (one on the top and the other at the bottom of the bearing height) and a set of mid-height multiple (radial) shear springs, all bound together by rigid links. The number of springs can be selected based on the accuracy/convergence of the numerical analysis. The axial behavior of the Multiple Axial Springs (each one representing an individual fiber of the bearing's cross-sectional area) is described by the nonlinear AxialSp uniaxial material, available in Opensees. The Multiple Shear Springs system consists of a series of identical springs arranged radially representing the isotropic behavior of the device in the horizontal plane. The nonlinear hysteretic behavior of shear springs is represented through the KikuchiAikenHDR material [13]. Buckling behavior due to high compressive load is simulated by the tilt of the rigid links and interaction between the shear and axial forces of the multiple axial and shear springs. The main advantage of the Kikuchi bearing element is represented by the possibility of capturing the axial-shear load interaction at small and large displacements, with consequent pre- and post- buckling behavior. On the other hand, the



implementation and computational efficiency of such model appears sometimes tricky and not always feasible. Moreover, cavitation and post cavitation behavior is not well captured. Finally, FSBs are modelled by a velocity-dependent and axial load-dependent friction law expressed as a function of the sliding friction coefficient at low (μ_{slow}) and fast (μ_{fast}) sliding velocities and axial load ratio. A nominal value of μ_{fast} equal to 1% for an axial load ratio of 1.0 has been considered. The dynamic-slow friction law has been assumed 2.5 times lower than μ_{fast} law, according to Cardone et al. [14].

The seismic performances of the case study building have been evaluated by means of multiple-stripe non-linear dynamic analyses (MSA) carried out considering 10 intensity levels and 20 ground motions per stripe [7]. Probabilistic seismic hazard analysis (PSHA) has been carried out using OPENQUAKE [15] to derive the hazard curve at the building site as a function of the Spectral acceleration $S_a(T)$, associated to the reference period (corresponding to the fundamental period of vibration of the case-study, $T = 3\text{sec}$). Hazard curve is further discretized at the ten IM values corresponding to the Return Periods: 10, 50, 100, 250, 500, 1000, 2500, 5000, 10000, 100000 years. Then, 20 Seismic records pairs have been selected for each IM based on the proper Conditional Mean Spectra (CMS), considering an appropriate Magnitudo-Distance-Deviation disaggregation and a suitable attenuation relationship for the building site. More details can be found in Iervolino et al. [15]. Failure modes and collapse conditions for the selected case study are summarized in Table 2. As can be seen, for each record, collapse is assumed to occur either if the superstructure or if the isolation system fails.

Table 2 – Failure modes and collapse conditions for base-isolated buildings

Failure modes		Collapse conditions RINTC (first edition) [7]	Collapse conditions RINTC (revised) [12]
Super structure	Ultimate ductility capacity	The relative displacement between the top of the building and the isolation level is equal to the top displacement from POA corresponding to a peak strength reduction of 50% on the negative slope.	
	Buckling	Axial compression force equal or greater than the critical buckling load.	Attainment of an axial compressive deformation equal or greater than 50%,
Isolation System	Cavitation	Attainment of an axial tensile deformation ϵ_t equal to or greater than 25%,	
	Shear	Attainment of a shear deformation γ equal to or greater than 350%	
	Maximum displacement capacity (for FSB)	Attainment of a horizontal displacement equal to or greater than the nominal displacement capacity of FSB plus half pot bearing diameter.	

For what concerns the superstructure, the collapse criteria is defined based on the roof drift value corresponding to a 50% drop from the maximum base-shear, computed via pushover analysis in each of the two horizontal directions [15]. On the other hand, the failure modes considered for HDRBs are cavitation, shear failure and buckling. It is worth noting that that failure modes and collapse conditions considered in the two editions of the RINTC research project [7, 12] are the same, except for the buckling collapse condition of HDRBs. As a matter of fact, in the first edition of RINTC research project [7] (using the HDR element), buckling is deemed to occur when the P/P_{cr} ratio between the current axial load and the critical buckling load is equal to 1, (P_{cr} is computed step by-step as a function of the effective shear rigidity and effective flexural rigidity of the device). In the recent review [12], where HDRBs are modeled with the Kikuchi bearing element, buckling is deemed to occur for an axial compressive strain of the order of 50%. Cavitation failure mode has been supposed to occur in the post-cavitation branch, for an axial tensile strain of the order of 25%.



For the shear failure, a limit shear strain equal to 350% has been considered. The failure of FSBs, instead, is associated to the attainment of a certain limit displacement, assumed equal to the displacement capacity of the device increased by an extra-displacement equal to a fraction (50%) of the bearing pot radius. The failure of the connections has been not considered, since the connection resistance must be (at least) two times greater than the maximum design shear force transmitted by the isolator, according to the European/Italian seismic Code [8]. All that considered, the collapse of the isolation system is assumed to occur when at least 50% of the isolation devices reaches (approximately at the same time) one of the failure modes described above. More details about the described assumptions can be found in Ragni et al. [7]. Fig. 1 shows the results obtained in [7] for the 6-storey base-isolated residential buildings located in L'Aquila (Soil C), assuming the collapse conditions reported in the first column of Table 2 and adopting the HDR model to describe the cyclic behavior of HDRBs. The results of Fig. 1 outline that failures are mainly due to buckling.

At this point, the conventional risk equation to evaluate the probability of collapse λ_c can be expressed as [6]:

$$\lambda_c = \int_0^{+\infty} P_f[\text{failure}|\text{IM} = x] |d\lambda_{\text{IM}}(x)| \quad (1)$$

where, λ_c is the mean annual frequency of collapse exceedance, briefly named as collapse risk, λ_{IM} is the seismic hazard function expressed in terms of mean annual frequency of exceedance (MAFE), corresponding to the Intensity Measure (IM), $P_f[\text{failure}|\text{IM}=x]$ represents the collapse fragility function. The latter, is usually expressed by the lognormal cumulative distribution function given two parameters: the median intensity causing collapse ($S_{a,c}$) and the corresponding standard deviation (β_c):

$$P_f[\text{failure}|\text{IM} = x] = \Phi \left[\frac{1}{\beta_c} \ln \frac{S_a(T)}{S_{a,c}} \right] \quad (2)$$

Assuming that the ground-motions corresponding to $\text{IM}(T_R) > \text{IM}(T_R=100000\text{yrs})$ will certainly cause failure, the mean annual failure rate (λ_c) can be conservatively approximated as [15]:

$$\lambda_c = \int_0^{100000} P_f[\text{failure}|\text{IM} = x] |d\lambda_{\text{IM}}(x)| + 10^{-5} \quad (3)$$

For the selected case study, a value of λ_c equal to 6.48×10^{-4} was obtained, which is about three times higher than the acceptable threshold suggested by the ASCE standards [4] (i.e. 2.0×10^{-4}). Such a value is probably due to the conventional buckling collapse condition assumed in [7], that appears too severe when compared to the others. To overcome this limitation, in the revised edition of the RINTC research project [12] the alternative Kikuchi model has been adopted. Fig. 2 shows the results obtained with the upgraded model. As can be seen, the collapse is solely due to the attainment of the ultimate displacement of FSBs, while the number of failures is slightly reduced as well as the value of λ_c , equal to 5.91×10^{-4} . A further reduction of the annual failure rate (of the order of 20%) can be obtained by enhancing the FSBs displacement capacity to a value greater than the displacement value associated to the ultimate shear strain of HDRBs (i.e., $\lambda_c = 4.72 \times 10^{-4}$). All that considered, it is worth noting that the mechanical model refinements and the critical reassessment of the collapse conditions do not significantly affect the results in terms of λ_c . In other words, despite the minimum requirements of the Italian seismic code ensure the acceptable level of safety, the resiliency objective suggested by the most advanced seismic codes is far from being achieved. As a consequence, a RTBD approach appears as the best solution to guarantee the mentioned resiliency objective.

3. Risk-target based design of base isolated building

The RTBD framework proposed for buildings with seismic isolation is inspired to previous works by Zizmond and Dolsek [16] for fixed-base buildings. Obviously, some adjustments are implemented to make the procedure by Zizmond and Dolsek suitable for base-isolated buildings. In the following section, the basis



of a RTBD approach for such specific buildings are summarized. The mentioned approach has been then applied to the selected case-study and validated through MSA. As reported in Section 2, the probability of collapse λ_C can be evaluated using Eq. (1) and Eq. (2). However, in the design phase, the structure is not identified and, as a consequence, the fragility function, hence the collapse risk, cannot be estimated. A step-by-step risk-targeted procedure is then needed. The procedure presented in the following develops in 5 main steps.

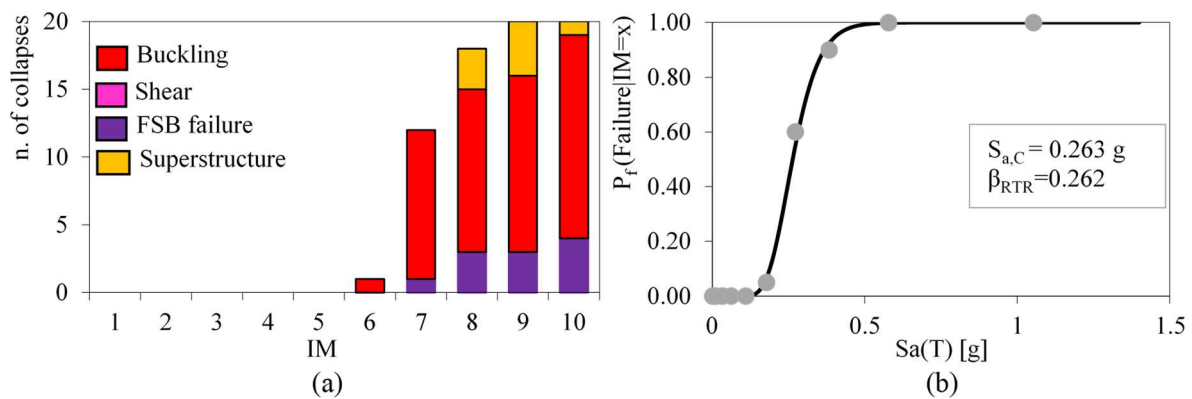


Fig. 1 – (a) Number of collapses for each IM and (b) corresponding collapse fragility curve obtained in the first edition of the RINTC research project [7]

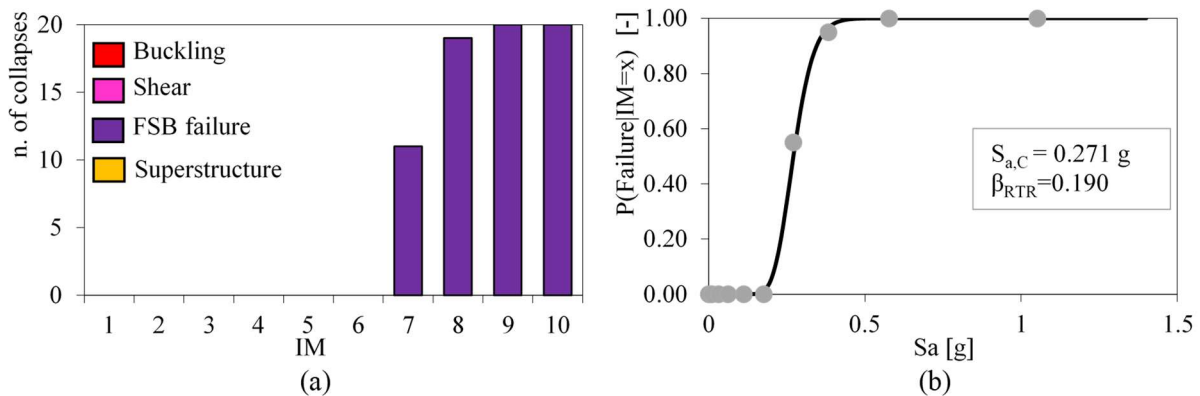


Fig. 2 – (a) Number of collapses for each IM and (b) corresponding collapse fragility curve obtained in the revised edition of the RINTC research project [12]

3.1 Step 1 – Definition of the acceptable collapse risk ($\lambda_{C,T}$)

In the first step, the target (acceptable) collapse risk $\lambda_{C,T}$ is defined. Different estimates (ranging from 10^{-5} to $2.0 \cdot 10^{-4}$ corresponding to a collapse probability of 0.1% to 1% in 50 years, respectively) of the acceptable collapse risk mean value are proposed in the literature for ordinary buildings. Herein, a target collapse rate of $2.0 \cdot 10^{-4}$ has been assumed according to Luco et al. [2].

3.2 Step 2 – Evaluation of the target median collapse spectral acceleration ($S_{a,c,T}$)

In the second step, the target median (50% probability of exceedance) collapse spectral acceleration corresponding to the fundamental period of the structure, $S_{a,c,T}$, is derived. For this purpose, some specific data or assumptions are required. First of all, the fundamental period of the structure ($T=T_{iso}$) should be set. Moreover, a proper value of the total dispersion ($\beta_{c,T}$) of the fragility curve should be assumed. The hazard curve of the building site is then needed. Assuming a linear representation of the seismic hazard function $H(S_a)$ in the log-space:

$$H(S_a) = k_0 S_a(T)^k \quad (4)$$



where k is the slope of the hazard function in the log-log domain, and k_0 is the annual rate of exceedance of $S_a(T)$ equal to 1 g, the probability of collapse λ_C can be evaluated as follows [6]:

$$\lambda_C = k_0 S_{a,C}^{-k} e^{\frac{k^2 \beta_{C,T}^2}{2}} \quad (5)$$

As a consequence, $S_{a,c,T}$ can be derived as:

$$S_{a,c,T} = \left(\frac{k_0}{\lambda_{C,T}} \right)^{\frac{1}{k}} e^{\frac{k \beta_{C,T}^2}{2}} \quad (6)$$

Different linearization approaches have been proposed in literature. As shown by Gkimprixis et al. [6], the best approximation is obtained using the linearization approach. In such approach, the hazard curve is fitted between the IM values corresponding to the targeted MAFE and the multiplied tenfold targeted MAFE, respectively. In order to account for different sources of uncertainty (record-to-record β_{rtr} , modeling β_m and uncertainty in collapse definition β_{ls}), a total standard deviation $\beta_{c,T}$ can be calculated using the Square Root of the Sum of the Squares (SRSS) rule:

$$\beta = \sqrt{\beta_{rtr}^2 + \beta_m^2 + \beta_{ls}^2} \quad (7)$$

Cardone et al. [17] showed that, for base isolated buildings, a record to record dispersion ranging between 0.2-0.3 can be assumed. Moreover, according to ATC-58 [18], the modeling dispersion can be assumed in the range 0.1 (i.e.: rigorous construction quality assurance, robust numerical model, failure modes explicitly modeled, ecc.) to 0.4 (i.e.: complete but schematic building design, idealized cyclic envelope curves failure modes not directly incorporated in the model), depending on the construction quality and quality/completeness of the numerical model. Finally, a value of β_{ls} equal to 0.2 has been proposed by Spillatura [1] for the uncertainty related to the collapse definition. All that considered, a total dispersion ranging between 0.3 and 0.8 is obtained, respectively.

3.3 Step 3 – Evaluation of the target median near-collapse spectral acceleration ($S_{a,c,T}$)

Collapse prevention is the main objective of any design. Adequate safety margin against collapse should be assured. Therefore, in the modern seismic codes, the Near Collapse (NC) limit state is considered for the safety verification towards collapse conditions. The transition between the collapse and NC limit state can be expressed through a reduction factor γ_{ls} , relating the median spectral acceleration causing collapse $S_{a,c,T}$ to the median spectral acceleration causing the NC limit state $S_{a,NC,T}$ of a structure:

$$\gamma_{ls} = \frac{S_{a,c,T}}{S_{a,NC,T}} \quad (8)$$

Zizmond and Dolsek [16] showed that for fixed based structures with period larger than T_C , the seismic intensity causing collapse is approximately 15% greater than that causing the NC limit state (i.e. $\gamma_{ls} = 1.15$). However, the value of γ_{ls} can significantly depend on the definition of the NC limit state and also on the structural typology. As mentioned in Section 2, for new buildings equipped with an hybrid isolation system (HDRBs + FPBs), the collapse condition for the isolation system depends on the typology and the associated failure modes of the isolation devices. For HDRBs, three collapse modes may occur, namely: (i) shear, (ii) buckling and (iii) tension. Sliders failure mode is due to the attainment of a horizontal displacement equal to the displacement capacity of the device increased by an over-stroke. All that considered, in the present study, the transition coefficient γ_{ls} has been calculated in terms of displacement assuming a constant value of the equivalent viscous damping and a direct proportionality between spectral acceleration intensities and response displacements, passing from Near Collapse to Collapse limit state. Considering the mentioned collapse failure modes of an hybrid isolation system the following general formulation is proposed:



$$\gamma_{ls} = \frac{\min(t_e \gamma_{max}; D_{ult}; D_{buck})}{D_{cap}} \quad (9)$$

where $t_e \gamma_{max}$ represent the collapse displacement associated to the attainment of the maximum shear deformation (γ_{max}) for an HDRB device featuring a rubber height equal to t_e ; D_{buck} represents the collapse displacement corresponding to the buckling failure (if buckling is expected to occur); D_{ult} is the collapse displacement capacity of FSBs; D_{cap} is the displacement capacity of the critical element of the isolation system (HDRB or FSB) at NC limit state. It is worth noting that for the sake of simplicity, the tensile failure of the HRDBs is not considered herein and the eventual collapse of the superstructure is neglected in first approximation.

Considering that at this step of the RT design procedure the isolation system is still unknown, a basic value of γ_{ls} should be chosen in first attempt. At the end of the procedure, once the isolation system has been effectively designed, a check on the assumed value of γ_{ls} can be performed to eventually repeat the process with the adjusted value of γ_{ls} . Based on the results reported in [7] and [12], corresponding to 4 case studies of new buildings equipped with hybrid isolation systems, first attempt values of γ_{ls} are proposed herein as a function of the prevalent failure mode. In particular, in case of shear failure, considering a (prudential) maximum shear deformation of 350% at collapse for HDRB, a lower bound value of γ_{ls} around 1.75 can be assumed. In case of FSB failure, values of γ_{ls} around 1.3-1.5 can be considered. Finally, values of γ_{ls} around 1.15-1.4 are expected if buckling collapse occurs. Clearly, once the transient coefficient γ_{ls} has been defined, $S_{a,NC,T}$ can be derived as follows:

$$S_{a,NC,T} = \frac{S_{a,C,T}}{\gamma_{ls}} \quad (10)$$

Finally, generally speaking, it could be useful to define the risk-targeted safety factor coefficient [16] relating the value $S_{a,NC,T}$ to the corresponding seismic demand defined by the traditional (code-based) uniform hazard maps for the associated limit state return period, T_R ($S_{a,TR}$):

$$\gamma_{im} = \frac{S_{a,NC,T}}{S_{a,TR}} \geq 1 \quad (11)$$

In the European/Italian seismic code, a return period of 975 years is typically associated to the collapse prevention limit state, for ordinary buildings. In order to respect the code limitation at the selected limit state, a lower bound of γ_{im} equal to 1 is proposed. The following relationship can be obtained by combining Eq. (10) with Eq. (11):

$$S_{a,NC,T} = \frac{S_{a,C,T}}{\gamma_{ls}} = \gamma_{im} S_{a,TR} \quad (12)$$

3.4 Step 4 – Evaluation of $S_{a,D,T}$ and $S_{d,D,T}$

A proper reduction factor r_{NC} is used to derive the design risk-targeted spectral acceleration $S_{a,D,T}$ from the 5%-damping elastic counterpart ($S_{a,NC,T}$). For fixed-base buildings, the reduction factor depends on the available ductility and overstrength ratio of the structure [16]. For based isolated buildings, r_{NC} can be assumed equal to $1/\eta$, where η is the damping reduction factor of the base-isolated building:

$$S_{a,D,T} = \frac{S_{a,NC,T}}{r_{NC}} = S_{a,NC,T} \eta \quad (13)$$

According to the seismic Italian/Eurocode, the damping reduction factor is expressed by the following relationship:

$$\eta = \sqrt{10 / (5 + \xi)} \quad (14)$$

Where ξ is the damping ratio of the isolation system.



The design spectral displacement can be then evaluated as:

$$S_{d,D,T} = \frac{S_{a,D,T}}{\omega^2} = S_{a,D,T} \left(\frac{T_{iso}}{2\pi} \right)^2 \quad (15)$$

3.5 Step 5 – Isolation system design

Once the fundamental period (T_{iso}) has been set (see Step 1) and the maximum displacement at the NC limit state ($S_{d,D,T}$) has been obtained, the design of the isolation system can be pursued. Assuming a reasonable value for the superstructure mass (M_{tot}), the total stiffness of the isolation system is obtained. Next, a suitable isolation device can be identified by entering the manufacturer's catalogues with the relevant displacement demand ($S_{d,D,T}$), the axial load capacity (from gravity load analysis) and the effective stiffness of the single device (K_{iso}). The latter can be evaluated as follows:

$$K_{iso} = \frac{M_{tot}}{N_{HDRB}} \left(\frac{2\pi}{T_{iso}} \right)^2 \quad (16)$$

Where N_{HDRB} is the number of elastomeric devices composing the hybrid isolation system.

3.6 Step 6 – Safety verifications

In the last step, the performances of the designed building are checked in accordance with the reference seismic code, by means of traditional structural analysis.

4. Application of risk-target based design

4.1 Design of the isolation system

The RTBD approach described in the previous section has been applied to the selected case study building (see Section 2), by assuming a risk-targeted value ($\lambda_{C,T}$) equal to $2.0 \cdot 10^{-4}$ and a target isolation period (T_{iso}) equal to 3 sec. The designed isolation system is constituted by 16 HDRBs plus 8FSBs, arranged below the perimeter and the inner columns of the building, respectively. The main characteristics of the RTBD designed isolation system are summarized in Table 1 (second line)

The results of the design procedure are summarized in Table 3. For the sake of clarity, the following assumptions have been made:

- Step 2: $S_{a,C,T}$ is evaluated with Eq. (6) interpolating the hazard curve between 1000 and 10000 years and assuming a total dispersion $\beta_{C,T}$ equal to 0.4 (considering the quality of the implemented numerical model and its capability of simulating most of the collapse mechanisms involved in the seismic response of the selected base-isolated building);
- Step 3: $S_{a,NC,T}$ is evaluated with Eq. (10) assuming $\gamma_{is}=1.75$. As a matter of fact, the collapse of the isolation system is dominated by the shear failure of HDRBs;
- Step 4: $S_{a,D,T}$ is evaluated with Eq. (13) assuming a damping ratio of the isolation system equal to 15%.

As can be seen from Table 3, the design displacement ($S_{d,D,T}$) at first iteration is equal to 414 mm. Considering the axial load capacity (derived from gravity load analysis) and the commercial catalogues of one of the main Italian manufacturers, only one device satisfies the design requirements (see Table 1) even if the displacement capacity appears slightly lower (400 mm). The corresponding coefficient γ_{is} for the selected HDRB results equal to 1.81. Consequently, repeating Step 2 and Step 4 assuming $\gamma_{is}=1.81$ (second iteration), the final value of $S_{d,D,T}$ is equal to 399 mm. Therefore, the selected device appears strictly adequate ($399\text{mm} < 400\text{mm}$). In line with the current practice and according to the Italian seismic code requirements [8], the sliding friction isolators (FPBs) should feature a displacement capacity at least 20% greater than the design displacement derived from the analysis, in order to account for possible residual displacements that may compromise the ultimate displacement capacity of not-recentring isolation systems [14]. As a consequence, such devices have been designed with a displacement capacity greater than that assumed for



the HDRBs (i.e. 450 mm). It is worth noting that the displacement capacity of FPBs is greater than that obtained in RINTC (450mm vs. 350 mm). Moreover, the HDRBs adopted in this study feature the same horizontal stiffness ($0.64 \times 16 = 10.24$ N/mm) of those adopted within the RINTC 2019 research project (more details in [12]). On the contrary, an enhanced displacement capacity of HDRBs has been obtained in the present study (i.e. 400 mm instead of 350 mm) leading to an increased value of the shear force transmitted to the superstructure. Obviously, in this condition, a premature collapse of the superstructure could be observed. Therefore, two different design sub-cases have been investigated: (i) superstructure designed using a behavior factor (q) equal to 1.5 (as in [7, 12]) and (ii) superstructure designed considering enhanced criteria (i.e. behavior factor equal to 1). Obviously, both sub-cases comply with the Italian seismic code requirements.

Table 3 – Application of the RTBD approach to the selected case-study building.

Step 1	Step 2	Step 3	Step 4
$\lambda_{c,T} = 2 \times 10^{-4}$	$\beta_{c,T} = 0.4$	$\gamma_{ls} = 1.75$	$\xi = 15\% \rightarrow \eta = \sqrt{10/(5 + \xi)} = 0.71$
$T_{iso} = 3.0$ s	$k_0 = 3.63 \times 10^{-5}$ $k = 1.84$	$\gamma_{im} = 1.48$	$S_{a,D,T} = S_{a,NC,T} \eta = 0.185g$
-	$S_{a,C,T} = \left(\frac{k_0}{\lambda_{c,T}}\right)^{\frac{1}{k}} e^{\frac{k\beta_{c,T}^2}{2}} = 0.46$ g	$S_{a,NC,T} = \frac{S_{a,C,T}}{\gamma_{ls}} = 0.26g$	$S_{d,D,T} = S_{a,D,T} \left(\frac{T_{iso}}{2\pi}\right)^2 = 0.414$ m
-	-	$\gamma_{ls} = 1.81$	$S_{a,D,T} = S_{a,NC,T} \eta = 0.179g$
-	-	$S_{a,NC,T} = \frac{S_{a,C,T}}{\gamma_{ls}} = 0.26g$	$S_{d,D,T} = S_{a,D,T} \left(\frac{T_{iso}}{2\pi}\right)^2 = 0.400$ m

4.2 Seismic risk and performance assessment

Multiple Stripe Analyses of the case-study building under consideration have been carried out to validate the proposed RTBD approach. For the sake of clarity, the modeling assumptions and the failure condition modes adopted herein are the same considered in the revised edition of the RINTC research project (i.e. Kikuchi bearing element, $q=1.5$, second column of Table 2). Fig. 3(a) shows the number of collapses and the failure modes associated to each examined IM. Fig. 3(b) shows the collapse fragility function thus obtained. As can be seen, by comparing Fig. 2(a) with Fig. 3(a), the number of collapse cases reduces, especially at IM7, passing from 10 to 2. As far as collapse modes is concerned, the number of collapse cases involving the superstructure increases. The latter result is twofold: first, the increased displacement capacity of the isolation system at the same period (i.e. stiffness) lead to a greater base shear transmitted to the superstructure; second, in some cases, even avoiding the collapse of the isolation system through the RTBD approach, the collapse of the superstructure follows, as second failure mode, in the analyses. The median value of the $S_{a,C}$ thus derived (see Fig. 3(b)) is equal to 0.356 g, which significantly differs from the expected value $S_{a,C,T}$, equal to 0.46 g shown in Table 3. The reason is that during the application of the RTBD procedure, the collapse of the superstructure is in first approximation neglected, while Fig 3(a) clearly shows that the collapse of the superstructure plays a not negligible role, especially because it has been designed assuming a behavior factor q equal to 1.5. Nevertheless, the value of the annual failure rate λ_c thus obtained is equal to 2.68×10^{-4} , which is pretty close to the target values selected at Step 1 of the RTBD process. As mentioned in section 4.1, in order to reduce the number of collapse cases and to better achieve the RTBD objective, the design of the superstructure has been repeated assuming enhanced criteria (i.e. behavior factor equal to 1). A new set of MSAs has been performed (see Fig. 4). As can be seen, the number of collapse cases involving the superstructure reduces, however new collapse cases involving the isolation system arise. In this condition, the value of the annual failure rate (λ_c) is equal to 1.97×10^{-4} , which perfectly matches the target value assumed at Step 1 of the RTBD procedure. From a practical point of view, the risk target objective has been attained increasing, by approximately 20%, the collapse displacement capacity obtained performing a “code-conforming design” and ensuring high performances of the superstructure, using a behavior factor equal to 1 in the design. It is worth noting that similar conclusions have been drawn by Constantinou et al.



[20] examining the collapse performance of US buildings equipped with FP isolators. It should be noted that the results of this study are site-specific and depend on the resulting risk-targeted safety factor γ_{im} at NC limit state ($\gamma_{im,NC}$). In principle, if $\gamma_{im,NC}$ results lower than 1, the target objective can be attained without increasing the collapse displacement of the isolation system (of the order of 20%) or the lateral strength of the superstructure ($q = 1$). Furthermore, it should be noted that in some cases, the risk-target safety factor $\gamma_{im,NC}$ already results significantly lower than 1 due to the (intentional or not) design choices of the designer.

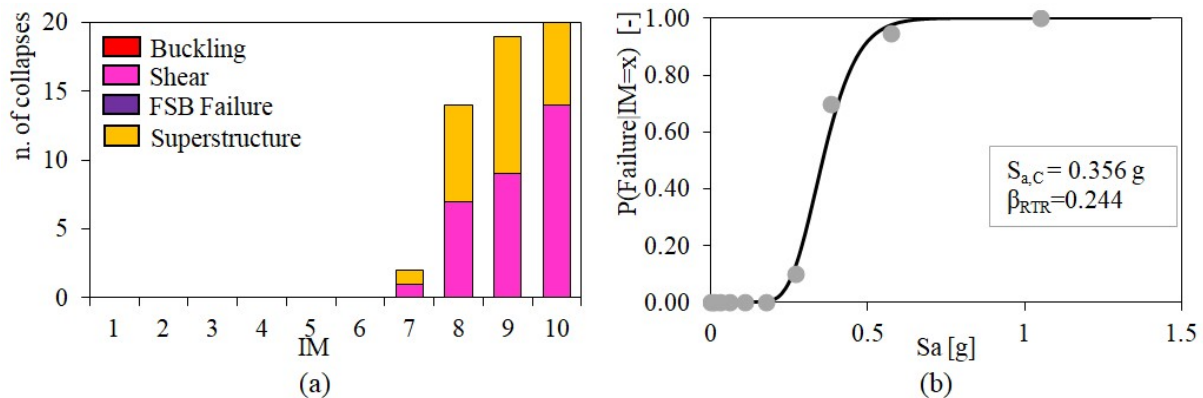


Fig. 3 – (a) Number of collapses for each IM and (b) corresponding collapse fragility curve for the selected case-study building (RTBD approach) assuming $q = 1.5$

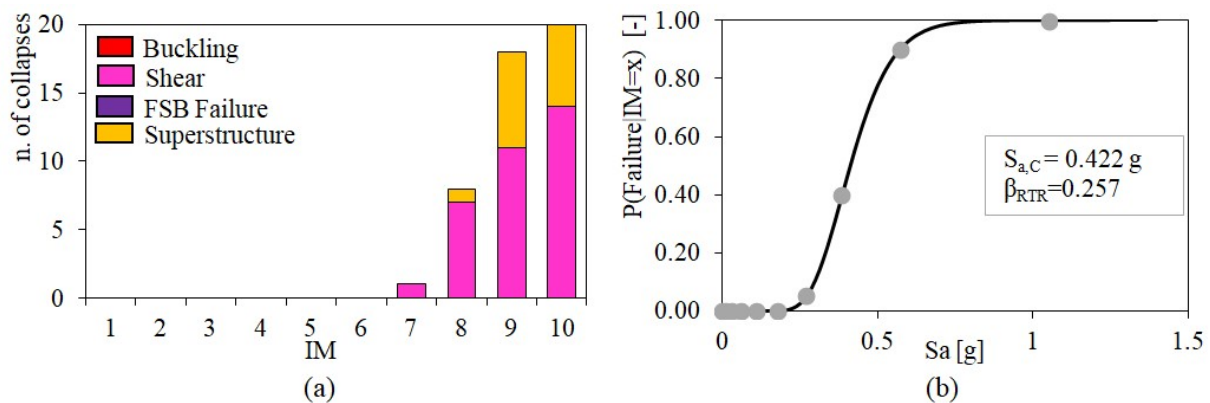


Fig. 4 – (a) Number of collapses for each IM and (b) corresponding collapse fragility curve for the selected case-study building (RTBD approach) assuming $q = 1.0$

6. Conclusions and future developments

The results of the RINTC project [7, 12], dealing with Italian code-conforming base-isolated buildings, outlined that the current design approach cannot guarantee an acceptable resilience objective in terms of probability of collapse, especially for high seismicity areas, based on the levels of risk of collapse that could be deemed acceptable based on the indications of past studies and requirements of other international codes. In this paper, a RTBD approach, inspired to previous works by Zizmond and Dolsek [16], has been developed for buildings with seismic isolation. The RTBD approach has been applied to a selected case-study representative of typical Italian residential RC buildings, assuming a target collapse rate of 2×10^{-4} . The validation of such approach has been performed through Multiple-Stripe analysis. This led to an annual failure rate of 1.97×10^{-4} , which fully comply with the target objective of the design. The preliminary results of this study also outline that following the using the Italian seismic code, the aforesaid risk-target design objective can be attained increasing, by approximately 20%, the design displacement of the isolation system and assuming a behavior factor of the superstructure equal to 1. Similar results and conclusions have been found by Constantinou et al. [19] considering US building designed by the ASCE/SEI 7 [4]. Clearly, the



results presented in this study are typology-dependent and site-specific. More case studies should be investigated in order to assess the applicability of the proposed RTBD approach.

Acknowledgements

The authors gratefully acknowledge the support of the ReLUIS Consortium for this research.

References

- [1] Spillatura A (2018): From record selection to risk targeted spectra for risk-based assessment and design. *Ph.D. Thesis, Istituto Universitario degli Studi Superiori (IUSS)*, Pavia, Italy.
- [2] Luco N, Ellingwood BR, Hamburger RO, Hooper JD, Kimballm JK, Kirchner CA (2007): Risk-targeted versus current seismic design maps for the conterminous United States. *SEAOC 2007 Convention Proceedings*, California.
- [3] ASCE (2010): Minimum design loads for buildings and other structures. *ASCE/SEI Standard 7-10. American Society of Civil Engineers ASCE*, Reston, USA.
- [4] ASCE (2017): Minimum design loads and associated criteria for buildings and other structures, *ASCE/SEI 7-16. American Society of Civil Engineers*, Reston, USA.
- [5] Douglas J, Ulrich T, Negulescu C (2013): Risk-targeted seismic design maps for mainland France. *Natural Hazards*, **65**(3), 1999-2013.
- [6] Gkimprixis A, Tubaldi E, Douglas J (2019): Comparison of methods to develop risk-targeted seismic design maps. *Bulletin of Earthquake Engineering*, 10.1007/s10518-019-00629-w.
- [7] Ragni L, Cardone D, Conte N, Dall'Asta A, Di Cesare A, Flora A, Leccese G, Micozzi F, Ponzo FC (2018): Modelling and Seismic Response Analysis of Italian Code-Conforming Base-Isolated Buildings. *Journal of Earthquake Engineering* **22**(2), 198-230.
- [8] DM. LL. PP. 17/01/2018: *Norme tecniche per le costruzioni (NTC2018)*. Rome, Italy (in italian).
- [9] McKenna F (2011): OpenSees: a framework for earthquake engineering simulation. *Computing in Science & Engineering*, **13**(4), 58–66.
- [10] Ibarra LF, Medina RA, Krawinkler H (2005): Hysteretic models that incorporate strength and stiffness deterioration. *Earthquake Engineering & Structural Dynamics* **34**(12), 1489–1511. doi:10.1002/eqe.495.
- [11] Kumar M, Whittaker A, Constantinou M (2014): An advanced numerical model of elastomeric seismic isolation bearings. *Earthquake Engineering & Structural Dynamics*, Published online, DOI: 10.1002/eqe.2431.
- [12] RINTC Workgroup (2019). Results of the 2019-2021 Implicit seismic risk of code-conforming structures in Italy (RINTC) project. *ReLUIS report, Rete dei Laboratori Universitari di Ingegneria Sismica (ReLUIS)*, Naples, Italy.
- [13] Ishii K, Kikuchi M (2018): Improved numerical analysis for ultimate behavior of elastomeric seismic isolation bearings. *Earthquake Engng Struct Dyn.* **48**, 65–77.
- [14] Cardone D, Gesualdi G, Brancato P (2015): Restoring capability of friction pendulum seismic isolation systems. *Bulletin of Earthquake Engineering*. **13**(8), 2449–2480.
- [15] Iervolino I, Spillatura A, Bazzurro P (2018): Seismic structural reliability of code-conforming Italian buildings. *Journal of Earthquake Engineering*, **22**(2), 5–27.
- [16] Žižmond J, Dolšek M (2019): Formulation of risk-targeted seismic action for the force-based seismic design of structures, *Earthquake engineering and structural dynamics*, **48**(12), 1406-1428.
- [17] Cardone D, Perrone G, Piesco V. Developing collapse fragility curves for base-isolated buildings. *Earthquake Engng Struct Dyn* 2019;48:78–102
- [18] ATC - Applied Technology Council FEMA P-58 (2012): Next-generation Seismic Performance Assessment for Buildings, Volume 1-2, 2012. *Federal Emergency Management Agency*, Washington D.C, USA.
- [19] Kitayama S, Costantinou MC (2018): Collapse performance of seismically isolated buildings designed by the procedures of ASCE/SEI 7. *Engineering Structures*. **164**, 243–258.